# Appendix A

# The equivalence of velocity-space DMO and Hale's DMO

In this appendix I prove the formal equivalence of the velocity-space DMO algorithm to the DMO method of Hale (1984). I first write the velocity-space algorithm in terms of its action on each dip component of the data. I then show how to recast Hale's algorithm in terms of dip decomposed data. This second part is based on the papers by Hale (1984) and Jakubowicz (1984). The formal difference between the methods then reduces to a change of order of two integrals.

The velocity-space algorithm can be summarized by the following sequence of steps: normal moveout (NMO) and stack over a range of velocities, dip decomposition of the stacks by two dimensional Fourier transformation, correction of the velocities by the cosine of the appropriate dip by shifting data between stacks, and inverse Fourier transformation. For medium of constant velocity $v$, the stacked, DMO-corrected image is found in the $v$ stack after the velocity corrections are applied. Call this image $q_{DMO}(t,y,v)$, where $t$ is time, $y$ is midpoint, and $v$ is the medium velocity. Before inverse transforming back to time and midpoint, the data is given by $q_{DMO}(\omega_0,k_y,v)$, where the subscript on the frequency $\omega_0$ is used to designate a zero offset frequency, for consistency with Hale's notation. Define a dip variable $D$ by

$$D \equiv \frac{k_y}{\omega_0} = \frac{2\sin\theta}{v} \tag{A.1}$$

where $\theta$ is the physical dip of an event. Also define an ideal narrow band dip filter operator $\mathbf{F}_D$ to select a specified dip component of the data:

$$\mathbf{F}_D \left[ q(\omega_0,k_y,v) \right] \equiv \begin{cases} q(\omega_0,k_y,v) & \text{if } k_y = \omega_0 D \\ 0 & \text{if } k_y \neq \omega_0 D \end{cases} . \tag{A.2}$$

The entire image can be recomposed by the superposition of all such dip components:

$$q_{DMO}(\omega_0,k_y,v) = \int dD \ \mathbf{F}_D \left[ q_{DMO}(\omega_0,k_y,v) \right] . \tag{A.3}$$

In the velocity-space DMO algorithm, each dip component of the DMO-corrected image is extracted from an appropriate constant-velocity stack, with the stacking velocity related to the medium velocity by equation (2.4), which in terms of $D$ becomes

$$v_\theta = v \left( 1 - \frac{D^2 v^2}{4} \right)^{-1/2} . \tag{A.4}$$

Call the data before this DMO correction $q_{stack}$. Then

$$q_{DMO}(\omega_0, k_y, v) = \int dD \; \mathbf{F}_D \left[ q_{stack}(\omega_0, k_y, v_\theta) \right] . \tag{A.5}$$

Transforming $\omega_0$ back to zero offset time $t_0$,

$$q_{DMO}(\omega_0, k_y, v) = \int dD \; \mathbf{F}_D \left[ \int dt_0 \, e^{i\omega_0 t_0} \, q_{stack}(t_0, k_y, v_\theta) \right] . \tag{A.6}$$

The stacked data $q_{stack}(t_0, k_y, v_\theta)$ is just an integral over offset $h$ of NMO-corrected data, with a moveout velocity of $v_{stack}$, so in terms of the original data $q(t, k_y)$,

$$q_{DMO}(\omega_0, k_y, v) = \int dD \; \mathbf{F}_D \left[ \int dt_0 \, e^{i\omega_0 t_0} \int dh \; q\left( t = (t_0^2 + 4h^2/v_\theta^2)^{1/2}, k_y, h \right) \right] \tag{A.7}$$

Hale's algorithm acts on transformed constant offset sections. In the notation of this chapter his algorithm is given by

$$q_{DMO}(\omega_0, k_y) = \int dh \int dt_n \, A^{-1} \, e^{iA\omega_0 t_n} \; q(t_n, k_y, h) , \tag{A.8}$$

where $t_n$ is the NMO-corrected time

$$t_n^2 = t^2 - \frac{4h^2}{v^2} \tag{A.9}$$

and

$$A = \left( 1 + \frac{h^2 k_y^2}{\omega_0^2 t_n^2} \right)^{1/2} . \tag{A.10}$$

The outer integral over offset $h$ is just the usual stack, so Hale's algorithm reduces to performing NMO, evaluating the indicated integral over $t_n$, and stacking over offset. The $t_n$ integral represents the DMO operator; leaving out this step gives the ordinary processing sequence of NMO and stack.

Hale's algorithm can also be decomposed in terms of its operation on individual dip components of the input data. Let $D$ and $\mathbf{F}_D$ be defined as above, and write

equation (A.8) as

$$q_{DMO}(\omega_0,k_y) = \int dD \;\; \mathbf{F}_D \left[ \int dh \int dt_n \, A^{-1} e^{iA\omega_0 t_n} \; q(t_n, k_y, h) \right] \tag{A.11}$$

where now

$$A = \left( 1 + \frac{h^2 D^2}{t_n^2} \right)^{1/2} . \tag{A.12}$$

The change of variables from $t_n$ to $t_0$ with

$$t_0^2 = t_n^2 + h^2 D^2 \tag{A.13}$$

has Jacobian

$$\frac{dt_n}{dt_0} = \left( 1 + \frac{h^2 D^2}{t_n^2} \right)^{1/2} = A \; . \tag{A.14}$$

This change of variables converts the integral in equation (A.11) into a Fourier transform over $t_0$ :

$$q_{DMO}(\omega_0,k_y) = \int dD \;\; \mathbf{F}_D \left[ \int dh \int dt_0 e^{i\omega_0 t_0} \, q_0(t_0=(t_n^2+h^2D^2)^{1/2}, k_y, h) \right] \tag{A.15}$$

where

$$q_0(t_0=(t_n^2+h^2D^2)^{1/2}, k_y, h) = q_{NMO}(t_n, k_y, h) \; . \tag{A.16}$$

Here the data with normal moveout applied at the medium velocity $v$ is written as $q_{NMO}$ and the data with the dip-corrected moveout velocity is written as $q_0$. To express $q_0$ in terms of the original recorded data $q$, note that

$$t^2 = t_n^2 + \frac{4h^2}{v^2} \tag{A.17}$$

$$= \left( t_0^2 - \frac{4h^2 \sin^2\theta}{v^2} \right) + \frac{4h^2}{v^2} \tag{A.18}$$

$$= t_0^2 + \frac{4h^2}{v^2} \cos\theta \tag{A.19}$$

$$= t_0^2 + \frac{4h^2}{v_\theta^2} \; . \tag{A.20}$$

Thus for a fixed dip component $\theta$

$$q_0(t_0,k_y,h) = q\left( \; t = (\, t_0^2 + 4h^2/v_\theta^2 \,)^{1/2}, k_y, h \right) \; . \tag{A.21}$$

Equation (A.15) then can be rewritten as

$$q_{DMO}(\omega_0,k_y,v) = \int dD\, \mathbf{F}_D \left[ \int dh \int dt_0\, e^{i\omega_0 t_0} q\Big( t = (t_0^2 + 4h^2/v_\theta^2)^{1/2}, k_y, h \Big) \right] . \quad \text{(A.22)}$$

Written this way, the only formal difference between the Hale algorithm, equation (A.22), and the velocity-space formulation, equation (A.7), is the interchange of order of the integral over offset $h$ (stacking) and the Fourier transform over $t_0$. Clearly, the two steps commute, so the methods are formally equivalent.

# Appendix B

## Computing the effective offset ratio $\gamma$ at zero offset

In section 3.4, I define the variable $\gamma$ to be equal to the surface offset $h$ divided by the effective subsurface offset $\mu(z_a)$. At zero offset, both $h$ and $\mu$ become zero, so $\gamma$ is indeterminate. However, the limit of $\gamma$ is well behaved as offset goes to zero, so $\gamma$ can be set equal to this limit without problem. This limit can always be evaluated numerically. In this appendix I derive an explicit expression for the case of vertically stratified media.

The simplest way to evaluate an indeterminate limit is to apply l'Hopital's rule, which states that the limit of a ratio is equal to the limit of the ratio of the derivatives of the numerator and denominator. Here I take the derivatives with respect to the ray parameter $p$. Consider the zero-offset ray from the subsurface point $\mathbf{d}=(x_d, z_d)$ to the surface, passing through the the anomaly point $\mathbf{a}=(x_a, z_a)$. Let $\theta(z)$ be the angle between the ray and vertical, so that $p = s(z)\sin\theta(z)$, where $s(z)$ is the slowness at depth $z$. Then the lateral position $x$ along a ray is given by

$$x = \int_{z_d}^{z} dz \tan\theta(z) \tag{B.1}$$

$$= \int_{z_d}^{z} \frac{p\,dz}{\sqrt{(s^2(z) - p^2}} \,. \tag{B.2}$$

Differentiating with respect to $p$ gives

$$\frac{dx}{dp}\Big|_z = \int_{z_d}^{z} \frac{d}{dp}\left[\frac{p\,dz}{\sqrt{s^2(z) - p^2}}\right] \tag{B.3}$$

$$= \int_{z_d}^{z} \frac{s^2(z)\,dz}{\left[s^2(z) - p^2\right]^{3/2}} \tag{B.4}$$

The value of $p$ corresponding to the zero-offset ray will be known from ray tracing. Then $h = x(z=0)$ and $\mu = x(z=z_a)$, so

$$\frac{h}{\mu} = \frac{\left.\frac{dx}{dp}\right|_{z=0}}{\left.\frac{dx}{dp}\right|_{z=z_a}} . \tag{B.5}$$

This value can be readily evaluated numerically.

The computation becomes even simpler for a constant slowness background. In that case the integrand in equation (B.4) is a constant that can be pulled outside the integrals and will cancel in the numerator and denominator of equation (B.5). So for constant slowness,

$$\frac{h}{\mu} = \frac{\int_{z_a}^{0} dz}{\int_{z_d}^{z_d} dz} = \frac{z_d}{(z_d - z_a)} \tag{B.6}$$

as used in equation (3.32) in the main text. Note that for constant slowness, the value of $h/\mu$ is independent of $p$ and depends only on the reflector and anomaly depths.

# Appendix C

## Decomposing the traveltime pyramid into dip components

In this appendix I show how to decompose the traveltime pyramid into dip components. Suppose the reflecting point $(x_d, z_d)$ lies on a bed a bed with dip $\theta$. Figure 3.5 shows the geometry of rays reflecting off such a dipping bed. Let $x$ be the point where the normal ray intersects the surface; in general $x$ will not coincide with the midpoint $y$. Let $t_1$ be the traveltime along the left leg of the ray, and $t_2$ the traveltime along the right leg. From the law of sines one has

$$\frac{x-s}{\sin\varsigma} = \frac{t_1}{\sin(\pi/2-\theta)} \tag{C.1}$$

and

$$\frac{g-s}{\sin\varsigma} = \frac{t_2}{\sin(\pi/2+\theta)} \tag{C.2}$$

where $s=y-h$ is the shot location and $g=y+h$ is the geophone location, and $\varsigma$ is the incident angle of the rays at the bed, measured from the normal. But $\sin(\pi/2-\theta)=\sin(\pi/2+\theta)=\cos\theta$, so equations (C.1) and (C.2) yield

$$\frac{x-s}{t_1} = \frac{g-x}{t_2} . \tag{C.3}$$

It follows that

$$x = \frac{gt_1+st_2}{t_1+t_2} \tag{C.4}$$

and

$$\tan\theta = \frac{x}{z_d} = \frac{g\sqrt{s^2+z_d^2} + s\sqrt{g^2+z_d^2}}{z_d\left(\sqrt{s^2+z_d^2} + \sqrt{g^2+z_d^2}\right)} . \tag{C.5}$$

Substituting $y=(g+s)/2$ and $h=(g-s)/2$ gives a relation for $\theta$, but it is awkward to solve for $y$ or $h$. A simpler relation can be found using double angles.

Referring to Figure 3.5 again, one has

$$\varsigma = \theta - \psi = \phi - \theta \tag{C.6}$$

so

$$\theta = \frac{1}{2}\,(\,\psi + \phi\,) \tag{C.7}$$

and

$$\tan(2\theta) = \tan(\,\psi + \phi\,) \tag{C.8}$$

$$= \frac{\tan\psi + \tan\phi}{1 - \tan\psi\tan\phi}\,. \tag{C.9}$$

Substituting

$$\tan\psi = \frac{y - x_d - h}{z_d} \tag{C.10}$$

and

$$\tan\phi = \frac{y - x_d + h}{z_d} \tag{C.11}$$

gives

$$\tan(2\theta) = \frac{2z_d\,(y - x_d)}{z_d^{\,2} - (y - x_d)^2 + h^{\,2}}\,. \tag{C.12}$$

This can be rewritten as

$$\frac{(y - x_d + z_d\cot 2\theta)^2}{z_d^{\,2}\csc^2 2\theta} - \frac{h^{\,2}}{z_d^{\,2}\csc^2 2\theta} = 1\,. \tag{C.13}$$

This can be recognized as the equation for a hyperbola with asymptotes

$$\pm h \;= y - x_d + \cot 2\theta \tag{C.14}$$

and foci

$$(h\,, y\,) = (\,0,\; x_d + z_d\,(\cot 2\theta \pm \sqrt{2}\csc 2\theta)\,)\,. \tag{C.15}$$

One can solve equation (C.13) for $h$ in terms of $y$ and $\theta$ to get

$$h_{\theta}^{\,2}\,(y\,) = (y - x_d + z_d\cot 2\theta)^2 - z_d^{\,2}\csc^2 2\theta \tag{C.16}$$

$$= (y - x_d\,)^2 + 2z_d\,(y - x_d\,)\cot 2\theta - z_d^{\,2}\,. \tag{C.17}$$

One could as well solve for $y$ to get

$$y_{\theta}(h\,) = x_d - z_d\cot 2\theta \pm \sqrt{h^{\,2} + z_d^{\,2}\csc^2 2\theta} \tag{C.18}$$

where the choice of sign will depend on whether $\theta>0$ or $\theta<0$. Note that $\theta=0$ must be considered separately; $h$ may then take on any value, but $y$ must always equal $x_d$; the two branches of the hyperbola collapse to one straight line.

These equations tell which $y$ and $h$ correspond to rays reflected off the dipping bed at the particular point $(x_d, z_d)$. This is the desired decomposition of the pyramid into contributions from different dips.

Only one of these rays will pass through a particular anomaly point $(x_a, z_a)$. The delta functions defined in equations (3.13) and (3.14) also give relations between allowable values of $y$ and $h$. Solving equation (C.17) and the appropriate one of these equations simultaneously will give the needed intersection point. The geometry of rays for the constant velocity case is analyzed in section 3.6. From equations (3.32) and (3.33) of that section, one has

$$h = | y - x_d - \gamma(x_a - x_d) | \tag{C.19}$$

where $\gamma = z_d/(z_d - z_a)$, and so

$$h^2 = (y - x_d)^2 - 2\gamma(x_a - x_d)(y - x_d) + \gamma^2(x_a - x_d)^2 . \tag{C.20}$$

From this and equation (C.17) one gets

$$2z_d(y - x_d)\cot 2\theta - z_d^2 = -2\gamma(x_a - x_d)(y - x_d) + \gamma^2(x_a - x_d)^2 . \tag{C.21}$$

Solving for $y$ gives

$$y = x_d + \frac{z_d^2 + \gamma^2(x_a - x_d)^2}{2[z_d \cot 2\theta + \gamma(x_a - x_d)]} . \tag{C.22}$$

(Note that $\theta=0$ is treated correctly as the limiting case of equation (C.22).) This gives $y$, and $h$ can then be found from equation (C.19):

$$h = \left| \frac{z_d^2 + \gamma^2(x_a - x_d)^2}{2[z_d \cot 2\theta + \gamma(x_a - x_d)]} - \gamma(x_a - x_d) \right| . \tag{C.23}$$

I note that the values of $h$, $y$, and $\theta$ which can be used in these equations are restricted. Both legs of the travel time path must be above the horizontal and must have equal incident angles; from this limitation one can show that, for positive $\theta$, one must have $\cot 2\theta > (x_d - x_a)/(z_d - z_a)$ and for negative $\theta$, $\cot 2\theta < (x_d - x_a)/(z_d - z_a)$.

In the text I discuss using $\partial\theta/\partial y$ and $\partial\varsigma/\partial h$ as weighting functions. The first of these is obtained by implicit differentiation of equation (C.12) to get

$$\frac{\partial\theta}{\partial y} = \frac{z_d\,(z_d^2 + (y - x_d)^2 + h^2)}{[\,z_d^2 - (y - x_d)^2 + h^2\,]^2 + 4z_d^2(y - x_d)^2} \tag{C.24}$$

$$= \frac{z_d\ (z_d{}^2+(y-x_d)^2+h^2)}{[\ z_d{}^2+(y-x_d)^2+h^2\ ]^2-4(y-x_d)^2h^2}\ . \tag{C.25}$$

To get the second, note that

$$\varsigma = \frac{1}{2}\ (\ \phi - \psi\ ) \tag{C.26}$$

and

$$\tan(2\varsigma) = \tan(\ \phi - \psi\ ) \tag{C.27}$$

$$= \frac{\tan\phi - \tan\psi}{1+\tan\phi\tan\psi}\ . \tag{C.28}$$

$$= \frac{2z_d\ h}{z_d{}^2+(y-x_d)^2-h^2}\ . \tag{C.29}$$

Interchanging the roles of $h$ and $(y-x_d)$ in this last equation yields exactly equation (C.12), so $\partial\varsigma/\partial h$ is exactly equal to $\partial\theta/\partial y$ as given in equation (C.24).

# Appendix D

## Comparing two methods for least-squares fitting of hyperbolas

In section 3.8 I derive Toldi's (1985) flat-dip operator as a special case of my more general operator. To do so, I used a particular set of weights in the fitting of a hyperbola to a set of traveltime data. In this appendix I show that this choice of weights is a consequence of the different approaches used to finding a best least squares fit. Suppose one is given a set of traveltimes that are perturbed away from an exact moveout hyperbola. There are two ways of setting up the problem of relating the change in the new best fitting hyperbola to the traveltime perturbations.

The first method is to use a $t^2$–$x^2$ linearizing parametrization, as Toldi (1985) does. The data to be fitted will be traveltimes $t(x)$ that will depend on the offset $h$. Write the equation for a hyperbola as

$$t^2 = \tau^2 + s^2 x^2 \tag{D.1}$$

where the slowness $s$ and the zero-offset traveltime $\tau$ are the fitting parameters to be found. In terms of the squared variables, equation (D.1) is a linear equation, and the best fitting values of $\tau^2$ and $s^2$ are given (e.g., Strang, 1980) by

$$s^2 = \frac{\sum_{j=1}^{N_x} \left( x_j^2 - \overline{x^2} \right) t_j^2}{\sum_{j=1}^{N_x} \left( x_j^2 - \overline{x^2} \right)^2} \tag{D.2}$$

and

$$\tau^2 = \frac{\sum_{j=1}^{N_x} \left( \overline{x^4} - x_j^2 \overline{x^2} \right) t_j^2}{\sum_{j=1}^{N_x} \left( x_j^2 - \overline{x^2} \right)^2} \tag{D.3}$$

where $\overline{x^2}$ and $\overline{x^4}$ are the second and fourth moments of the data defined by

$$\overline{x^2} = \frac{1}{N_x} \sum_{j=1}^{N_x} x_j^2 \tag{D.4}$$

and

$$\overline{x^4} = \frac{1}{N_x} \sum_{j=1}^{N_x} x_j^4 \,. \tag{D.5}$$

Perturb the values of $t_j$, $s$ and $\tau$ and drop all higher order terms to get

$$\Delta s = \frac{1}{s} \frac{\sum_{j=1}^{N_x} \left( x_j^2 - \overline{x^2} \right) t_j \, \Delta t_j}{\sum_{j=1}^{N_x} \left( x_j^2 - \overline{x^2} \right)^2} \tag{D.6}$$

and

$$\Delta \tau = \frac{1}{\tau} \frac{\sum_{j=1}^{N_x} \left( \overline{x^4} - x_j^2 \overline{x^2} \right) t_j \, \Delta t_j}{\sum_{j=1}^{N_x} \left( x_j^2 - \overline{x^2} \right)^2} \,. \tag{D.7}$$

Another approach is to expand around the original hyperbola and solve a set of linear equations in the perturbations. This is the approach I used in this dissertation, because no linearizing parametrization is available for the double-square-root equation (3.7). In this method one writes the set of linearized approximate equations

$$\Delta t_j \approx \frac{\partial t_j}{\partial s} \Delta s + \frac{\partial t_j}{\partial \tau} \Delta \tau \,. \tag{D.8}$$

The least squares solution to these equations is given in equations (3.49) to (3.52). To compare these values with equations (D.6) and (D.7) one needs to evaluate each of the inner products in the equations from chapter 3. Start with equation (3.46) for the partial derivatives of $t$ (dropping the ubiquitous subscript $d$):

$$t_s = \frac{2sh^2}{\sqrt{\tau^2/4 + s^2 h^2}} = \frac{sx^2}{t} \tag{D.9}$$

and

$$t_\tau = \frac{\tau}{2\sqrt{\tau^2/4 + s^2 h^2}} = \frac{\tau}{t} \tag{D.10}$$

where I have changed from the half offset $h$ to the full offset $x = 2h$ to agree with the notation of equations (D.6) and (D.7). Let the weighting function

$\alpha = z^2 + h^2 = t^2/4s^2$. Then

$$\mathbf{t}_s \cdot \mathbf{t}_\tau = \sum_{j=1}^{N_x} \alpha(x_j)\, t_s(x_j)\, t_\tau(x_j) \tag{D.11}$$

$$= \sum_{j=1}^{N_x} \frac{t_j^2}{4s^2}\, \frac{s x_j^2}{t_j}\, \frac{\tau}{t_j} \tag{D.12}$$

$$= \frac{\tau}{4s} \sum_{j=1}^{N_x} x_j^2 \tag{D.13}$$

$$= \frac{N_x \tau \overline{x^2}}{4s} \,. \tag{D.14}$$

Similarly,

$$\mathbf{t}_s \cdot \mathbf{t}_s = \sum_{j=1}^{N_x} \frac{t_j^2}{4s^2}\, \frac{\tau}{t_j}\, \frac{\tau}{t_j} \tag{D.15}$$

$$= \frac{N_x \overline{x^4}}{4} \tag{D.16}$$

and

$$\mathbf{t}_\tau \cdot \mathbf{t}_\tau = \sum_{j=1}^{N_x} \frac{t_j^2}{4s^2}\, \frac{s x_j^2}{t_j}\, \frac{s x_j^2}{t_j} \tag{D.17}$$

$$= \frac{N_x \tau^2}{4s^2} \,. \tag{D.18}$$

Then one has

$$\Delta s = \mathbf{A}_s \cdot \Delta \mathbf{t} \tag{D.19}$$

$$= \sum_{j=1}^{N_x} \frac{\alpha(x_i) \left[ (\mathbf{t}_\tau \cdot \mathbf{t}_\tau) t_s(x_i) - (\mathbf{t}_s \cdot \mathbf{t}_\tau) t_\tau(x_i) \right] \Delta t_i}{(\mathbf{t}_s \cdot \mathbf{t}_s)(\mathbf{t}_\tau \cdot \mathbf{t}_\tau) - (\mathbf{t}_s \cdot \mathbf{t}_\tau)^2} \tag{D.20}$$

$$= \sum_{j=1}^{N_x} \frac{\dfrac{t_j^2}{4s^2} \left[ \dfrac{N_x \tau^2}{4s^2} \dfrac{s x_j^2}{t_j} - \dfrac{N_x \tau \overline{x^2}}{4s} \dfrac{\tau}{t_j} \right] \Delta t_j}{\dfrac{N_x \overline{x^4}}{4} \dfrac{N_x \tau^2}{4s^2} - \dfrac{N_x \tau \overline{x^2}}{4s} \dfrac{N_x \tau \overline{x^2}}{4s}} \tag{D.21}$$

$$= \frac{1}{s} \frac{\sum_{j=1}^{N_x} \left( x_j^2 - \overline{x^2} \right) t_j \Delta t_j}{N_x \left[ \overline{x^4} - (\overline{x^2})^2 \right]} \,. \tag{D.22}$$

Similarly,

$$\Delta\tau = \mathbf{A}_\tau \cdot \Delta\mathbf{t} \tag{D.23}$$

$$= \sum_{j=1}^{N_x} \frac{\alpha(x_i)\left[ (\mathbf{t_s}\cdot\mathbf{t_s})t_\tau(x_i) - (\mathbf{t_s}\cdot\mathbf{t}_\tau)t_s(x_i) \right]\Delta t_i}{(\mathbf{t_s}\cdot\mathbf{t_s})(\mathbf{t}_\tau\cdot\mathbf{t}_\tau) - (\mathbf{t_s}\cdot\mathbf{t}_\tau)^2} \tag{D.24}$$

$$= \sum_{j=1}^{N_x} \frac{\frac{t_j^2}{4s^2}\left[ \frac{N_x\,\overline{x^4}}{4}\frac{\tau}{t_j} - \frac{N_x\,\tau\,\overline{x^2}}{4s}\frac{sx^2}{t_j} \right]\Delta t_j}{\frac{N_x\,\overline{x^4}}{4}\frac{N_x\,\tau^2}{4s^2} - \frac{N_x\,\tau\,\overline{x^2}}{4s}\frac{N_x\,\tau\,\overline{x^2}}{4s}} \tag{D.25}$$

$$= \frac{1}{\tau}\frac{\sum_{j=1}^{N_x}\left( \overline{x^4} - x_j^2\overline{x^2} \right)t_j\,\Delta t_j}{N_x\left[ \overline{x^4} - (\overline{x^2})^2 \right]} . \tag{D.26}$$

Equations D.22 and D.26 are identical to D.6 and D.7 except for the different appearence of the denominators. However, they are really the same, as I now show.

$$\sum_{j=1}^{N_x}\left( x_j^2 - \overline{x^2} \right)^2 = \sum_{j=1}^{N_x}\left[ x_j^4 - 2x_j^2\overline{x^2} + (\overline{x^2})^2 \right] \tag{D.27}$$

$$= N_x\,\overline{x^4} - 2N_x(\overline{x^2})^2 + N_x(\overline{x^2})^2 \tag{D.28}$$

$$= N_x\left[ \overline{x^4} - (\overline{x^2})^2 \right] . \tag{D.29}$$

So the two denominators are the same, and the two least squares methods give the same results with the particular weighting chosen.

# Appendix E

## An alternative algorithm for nonlinear inversion

In section 4.5 I present an algorithm for inverting migration slownesses for interval slowness. That algorithm assumes that a grid of reflecting points **d** with fixed locations $(x_d, z_d)$ was used throughout. For reasons discussed in that section, it might be preferable to use a fixed grid $(y_d, \tau_d)$ in the data and let the reflector locations $(x_d, z_d)$ that map to these data grid points vary with successive iterations. The operator **G**, however, is defined relative to a fixed location $(x_d, z_d)$. What one needs is to know how the migration slowness $s_d$ changes for a fixed data location $(y_d, \tau_d)$ when the interval slowness model **m** is perturbed. Changing the model **m** causes a given reflecting point to appear at a different $(y, \tau)$, so one needs to compute not just how $s_d$ changes, but also which reflecting point it represents in the updated model. Let primes indicate the perturbed model, so the reflecting point associated with $s(y, \tau)$ is associated with $s'(y', \tau')$ for the new model. Let $\Delta s = s' - s$, $\Delta y = y' - y$, and $\Delta \tau = \tau' - \tau$. Also, let the partial derivatives of $s$ relative to a fixed $(y, \tau)$ be denoted by $\frac{\delta s}{\delta m}$, etc and let the partial derivatives relative to a fixed reflecting location $(x, z)$ be indicated by the usual partial derivative notation $\frac{\partial s}{\partial m}$, etc. Then one has

$$s'(y', \tau') \approx s(y, \tau) + \sum_a \frac{\partial s}{\partial m_a} \Delta m_a \quad . \tag{E.1}$$

Also to first order, one has,

$$\left. \frac{\delta s'}{\delta y'} \right|_{(y', \tau')} \approx \left. \frac{\delta s}{\delta y} \right|_{(y, \tau)} \tag{E.2}$$

and

$$\left. \frac{\delta s'}{\delta \tau'} \right|_{(y', \tau')} \approx \left. \frac{\delta s}{\delta \tau} \right|_{(y, \tau)} . \tag{E.3}$$

One can then write

$$s'(y,\tau) \approx s'(y'-\Delta y,\tau'-\Delta\tau) \tag{E.4}$$

$$\approx s'(y',\tau') - \left.\frac{\delta s'}{\delta y'}\right|_{(y',\tau')} \Delta y - \left.\frac{\delta s'}{\delta \tau'}\right|_{(y',\tau')} \Delta\tau \tag{E.5}$$

$$\approx s(y,\tau) + \sum_a \frac{\partial s}{\partial m_a}\,\Delta m_a - \left.\frac{\delta s}{\delta y}\right|_{(y,\tau)} \Delta y - \left.\frac{\delta s}{\delta \tau}\right|_{(y,\tau)} \Delta\tau \tag{E.6}$$

$$\approx s(y,\tau) + \sum_a \frac{\partial s}{\partial m_a}\,\Delta m_a - \frac{\delta s}{\delta y}\sum_a \frac{\partial y}{\partial m_a}\,\Delta m_a - \frac{\delta s}{\delta \tau}\sum_a \frac{\partial \tau}{\partial m_a}\,\Delta m_a \tag{E.7}$$

Thus

$$\frac{\delta s_d}{\delta m_a} = \frac{\partial s_d}{\partial m_a} - \frac{\delta s_d}{\delta \tau_d}\,\frac{\partial \tau_d}{\partial m_a} - \frac{\delta s_d}{\delta y_d}\,\frac{\partial y_d}{\partial m_a} \tag{E.8}$$

$$= \mathbf{G}_s(\mathbf{d},\mathbf{a}) - \frac{\delta s_d}{\delta \tau_d}\,\mathbf{G}_\tau(\mathbf{d},\mathbf{a}) - \frac{\delta s_d}{\delta y_d}\,\mathbf{G}_y(\mathbf{d},\mathbf{a}) \tag{E.9}$$

$$\equiv \mathbf{H}(\mathbf{d},\mathbf{a})\,. \tag{E.10}$$

The function $\mathbf{H}$ as defined here provides the gradient direction needed for an iterative inversion. The derivatives of $s$ with respect to $\tau$ and $y$ can be evaluated by finite differences. The second and third terms in equations (E.8) and (E.9) compensate for the change in the particular reflecting point $(x_d, z_d)$ that is being mapped into the data space coordinates $(y_d, \tau_d)$ at each iteration. The magnitude of these terms depends on the derivative of the slowness field. Against a constant slowness background they are identically zero, and for any smooth slowness function, they will be small.

The objective function $Q$ is defined as in equation 4.3,

$$Q(\mathbf{s}) \equiv \sum_{\mathbf{d}} E\left[s_d(y_d,\tau_d), y_d, \tau_d\right]. \tag{E.11}$$

The gradient of $Q$ with respect to the interval slowness model $\mathbf{m}$ is now given by

$$(\nabla_{\mathbf{m}} Q)_a = \frac{\partial Q}{\partial m_a} = \sum_{\mathbf{d}} \frac{\partial Q}{\partial s_d}\,\frac{\delta s_d}{\delta m_a} \tag{E.12}$$

or

$$\nabla_{\mathbf{m}} Q = \mathbf{H}^T \nabla_{\mathbf{s}} Q\,. \tag{E.13}$$

The derivatives of $Q$ with respect to the migration slowness $s_d$ can be computed as before by finite differences.

A steepest ascent optimization algorithm using this new gradient can now be outlined as follows:

Set initial interval slowness model $\mathbf{m}$
Set initial values of $\mathbf{s}_d$ on a fixed grid of $(y_d, \tau_d)$
Set initial values of $(x_d, z_d)$ corresponding to $(y_d, \tau_d)$ grid.
Calculate initial dip spectrum estimate $\theta_d$ from time dips and $\mathbf{s}_d$
Compute $\mathbf{G(d,a)}$ and $\mathbf{H(d,a)}$ from initial $\mathbf{m}$, $\mathbf{s}$, and $\theta_d$

Repeat until $\Delta Q$ is small enough
{

1. Compute $\nabla_{\mathbf{s}} Q$ by finite differences
2. Form $\nabla_{\mathbf{m}} Q = \mathbf{H}_s^T \nabla_{\mathbf{s}} Q$
3. Line search for $\alpha$ that maximizes $Q(\mathbf{m}+\alpha\nabla_{\mathbf{m}} Q) = Q(\mathbf{s}+\alpha\mathbf{H}\nabla_{\mathbf{m}} Q)$
4. Update model
   $\Delta\mathbf{m} = \alpha\nabla_{\mathbf{m}} Q$
   $\mathbf{m} = \mathbf{m} + \Delta\mathbf{m}$
   $\mathbf{s} = \mathbf{s} + \mathbf{H}\Delta\mathbf{m}$
5. Update map between $(y_d, \tau_d)$ and $(x_d, z_d)$
   $\mathbf{y} = \mathbf{y} + \mathbf{G}_{\mathbf{y}}\Delta\mathbf{m}$
   $\tau = \tau + \mathbf{G}_{\tau}\Delta\mathbf{m}$
   Compute new $\mathbf{x}$,$\mathbf{z}$ by inverse interpolation
6. Update $\theta_d$
7. Compute new $\mathbf{G(d,a)}$ and $\mathbf{H(d,a)}$ for new $\mathbf{m}$, $\mathbf{s}$, and $\theta_d$

}

This algorithm is similar in many ways to that of section 4.5. The important point to note is that $H$ here relates perturbations on a fixed grid of model points $\mathbf{m(a)}$ to perturbations again on a fixed grid in data space $\mathbf{s(d)}$. The migration slownesses $\mathbf{s}$ are explicitly treated as a function of the coordinates $y$ and $\tau$. Thus the objective function $Q$ is always evaluated by a sum over the same grid points $\mathbf{d}=(y_d, \tau_d)$. Likewise, the finite difference approximations to the derivatives are always calculated at the same $(y_d, \tau_d)$ values. Note that, like the alogrithm of section 4.5, this approach can also be modified to use ray tracing to update the map between $(x_d, z_d)$ and $(y_d, \tau_d)$ and to use DMO slownesses instead of migration slownesses.

The choice between this algorithm and that of section 4.5 is somewhat analogous to the choice between Lagrangian or Eulerian viewpoints in fluid dynamics. A similar problem arises there, requiring a choice between computing spatial gradients at a fixed location (Eulerian) or for a particular particle (Lagrangian). (For introductory discussion of the Eulerian and Lagrangian approaches in mechanics, see Batchelor (1967) or Aki and Richards (1980).) Here the choice is between evaluating gradients for a fixed location in the $(y, \tau)$ data space or for a fixed reflecting point in $(x, z)$ space.

I do not know which approach is better to use for practical implementation. The approach presented in this appendix is perhaps easier to implement, in so much as it works with the migration slowness data on the grid on which it is provided. This is a major advantage, as it allows one to decrease the size of the problem by using only those parts of the data that correspond to strong reflectors without knowing in advance the correct physical locations of these reflectors. However, problems could arise with this algorithm because of the inverse interpolation step needed to update the map between $(x, z)$ and $(y, \tau)$. This map could fail to be one-to-one, or, if the model space is chosen badly, parts of the data could be left wholly outside the image of the model space. In either of these cases it would be impossible to figure out which $(x, z)$ to associate with a given $(y, \tau)$. The approach of section 4.5 should have no such problem, as it works in principle only with the map from $(x, z)$ to $(y, \tau)$ and not the inverse; it would simply count a contribution from some $(x, z)$ more than once in calculating the objective function if that point maps onto multiple values of $(y, \tau)$, and would never look at those parts of the data that are not images of some part of the model space. The two approaches thus interact with the data and model differently. The objective function calculation in the algorithm of this appendix weights all parts of the data equally, without concern for whether they are actually well determined by the given model. The method of section 4.5, on the other hand, ignores those parts of the data that are not the images of any point in the data, and may allow some parts of the data to contribute much more than others.

# Appendix F

## The movement of reflectors during migration

In this appendix I derive equations for the movement of reflectors during migration with different velocities. Start with a point $(x,z)$ on a reflector that has dip angle $\theta$ from the horizontal. If the medium has a constant slowness $s$, this point appears in zero-offset data at midpoint $y$ and time $t$ given by

$$y = x - z\tan\theta \tag{F.1}$$

and

$$t = 2sz\sec\theta\ . \tag{F.2}$$

The apparent dip (time-dip) of this reflecting segment is

$$\frac{dt}{dy} = -2s\sin\theta\ . \tag{F.3}$$

Suppose now that this reflector segment is migrated with a slowness $s'$. The dip $\theta'$ in the resulting $(x',z')$ section is given by

$$\sin\theta' = \frac{-1}{2s'}\frac{dt}{dy} \tag{F.4}$$

$$= \frac{s}{s'}\sin\theta\ . \tag{F.5}$$

The new values of $x'$ and $z'$ are found by solving equations (F.1) and (F.2). Here $y$ and $t$ are given, but $\theta'$ varies with $s'$. One has

$$z' = \frac{t}{2s\sec\theta'} \tag{F.6}$$

$$= \frac{t}{2s}\cos\theta' \tag{F.7}$$

$$= \frac{t}{2s}\sqrt{1-\sin^2\theta'} \tag{F.8}$$

$$= \frac{t}{2s}\sqrt{1-\frac{s^2}{(s')^2}\sin^2\theta} \tag{F.9}$$

and

$$x' = y + z' \tan\theta' \tag{F.10}$$

$$= y + \frac{t}{2s'} \cos\theta' \tan\theta' \tag{F.11}$$

$$= y + \frac{t}{2s'} \sin\theta' \tag{F.12}$$

$$= y + \frac{ts}{2(s')^2} \sin\theta \, . \tag{F.13}$$

In practice time migration results are expressed not in the coordinates $(x',z')$ but in migrated midpoint $y'$ and migrated time $\tau'$, where $y'=x'$ and $\tau'=2s'z'$. Solving for $y'$ and $\tau'$ in terms of $x$ and $z$ yields

$$\tau' = t \sqrt{1 - \frac{s^2}{(s')^2} \sin^2\theta} \tag{F.14}$$

$$= 2sz \sqrt{1 - \frac{s^2}{(s')^2} \sin^2\theta} \tag{F.15}$$

and

$$y' = y + \frac{ts}{2(s')^2} \sin\theta \tag{F.16}$$

$$= x - z \tan\theta + \frac{zs^2}{2(s')^2} \tan\theta \tag{F.17}$$

$$= x - z \tan\theta \left( 1 - \frac{s^2}{2(s')^2} \right) . \tag{F.18}$$

These are the equations used in chapter 4 for tracking the $(y,\tau)$ image of a reflecting point $(x,z)$ as migration slowness changes.

In section 2.6 limits on the motion of reflectors are used to estimate the necessary density for sampling slowness. Differentiating equations (F.140 and (F.16) gives

$$\frac{dy}{ds} = \frac{-ts}{(s')^3} \sin\theta \tag{F.19}$$

and

$$\frac{d\tau}{ds} = \frac{t \sin^2\theta}{\sqrt{1 - \frac{s^2}{(s')^2} \sin\theta}} \frac{s^2}{(s')^3} \, . \tag{F.20}$$

In estimating sampling density one does not know $s$ a priori, so one sets $s'=s$. Then these last two equations reduce to

$$\frac{dy}{ds} = \frac{-t}{s^2} \sin\theta \tag{F.21}$$

and

$$\frac{d\,\tau}{ds} = \frac{t}{s}\,\sin\theta\,\tan\theta \tag{F.22}$$

which are the equations used in section 2.6.

## REFERENCES


Aki, K., and Richards, P., 1980, Quantitative seismology: Freeman.

Al-Chalabi, M., 1974, An analysis of stacking, rms, average, and interval velocities over a horizontally layered ground: Geophysical Prospecting, **22**, 458-475.

Al-Chalabi, M., 1979, Velocity determination from seismic reflection data, *in* Fitch, A.A., Ed., Developments in geophysical exploration methods 1: Applied Science Publ., Ltd., 1-68.

Al-Yahya, K.M., 1987, Velocity analysis by iterative profile migration: Ph.D. thesis, Stanford University (SEP-53).

Batchelor, 1967, An introduction to fluid dynamics: Cambridge Univ. Press.

Bishop, T.N., Bube, K.P., Cutler, R.T., Langan, R.T., Love, P.L., Resnick, J.R., Shuey, R.T., Spindler, D.A., and Wyld, H.W., 1985, Tomographic determination of velocity and depth in laterally varying media: Geophysics, **50**, 903-923.

Bolondi, G., Loinger, E., and Rocca, F., 1982, Offset continuation of seismic sections: Geophysical Prospecting, **30**, 813-828.

Chiu, S.K.L., Kanasewich, E.R., and Phadke, S., 1986, Three-dimensional determination of structure and velocity by seismic tomography: Geophysics, **51**, 1559-1571.

Chun, J.H., and Jacewitz, C.A., 1978, A fast multi-velocity function frequency domain migration: Presented at 48th annual SEG meeting, San Francisco.

Claerbout, J.F., 1976, Fundamentals of geophysical data processing: McGraw-Hill.

Claerbout, J.F., 1984, Imaging the Earth's interior: Blackwell Scientific Publications Ltd.

Cordier, J.-P., 1985, Velocities in reflection seismology: D. Reidel Publ. Co.

De Vries, D., and Berkhout, A.J., 1984, Velocity analysis based on minimum entropy: Geophysics, **49**, 2132-2142.

Deregowski, S.M., 1986, What is DMO?: First Break, **4**, 7-24.

Deregowski, S.M., and Brown, S.M., 1983, A theory of acoustic diffractors applied to 2-D models: Geophysical Prospecting, **31**, 293-333.

Deregowski, S.M., and Rocca, F., 1981, Geometrical optics and wave theory of constant offset sections in layered media: Geophysical Prospecting, **29**, 374-406.

Dix, C.H., 1955, Seismic velocities from surface measurements: Geophysics, **20**, 68-86.

Etgen, J., 1988, Velocity analysis by prestack depth migration: linear theory: SEP-57, 77-98.

Gibson, B., Larner, K., and Levin, S., 1983, Efficient 3-D migration in two steps: Geophysical Prospecting, **31**, 1-33.

Gill, P.E., Murray, W., and Wright, M.H., 1981, Practical optimization: Academic Press.

Golub, G.H., and Van Loan, C.F., 1983, Matrix computations: Johns Hopkins.

Gray, W.C., 1985, U.S. Patent 4,479,205, appl. 11/16/1981, iss. 10/23/84: Geophysics, **50**, 511.

Gray, W.C., and Golden, J.E., 1983, Velocity determination in a complex earth: Presented at the 53rd annual SEG meeting, in Las Vegas

Hale, D., 1983, Dip moveout by Fourier transform: Ph.D. thesis, Stanford University.

Hale, D., 1984, Dip moveout by Fourier transform: Geophysics, **49**, 741-757.

Harlan, W.S., Claerbout, J.F., and Rocca, F., 1984, Signal/noise separation and velocity estimation: Geophysics, **49**, 1869-1880.

Hatton, L., Larner, K.L., and Gibson, B.S., 1981, Migration of seismic data from inhomogeneous media: Geophysics, **46**, 751-767.

Hatton, L., Worthington, M.H., and Makin, J., 1986, Seismic data processing: theory and practice: Blackwell Scientific Publications.

Hubral, P., 1977, Time migration - some ray theoretical aspects: Geophysical Prospecting, **25**, 738-745.

Hubral, P., and Krey, T., 1980, Interval velocities from seismic reflection time measurements: Society of Exploration Geophysicists.

Jakubowicz, H., 1984, A simple efficient method of pre-stack partial migration: Presented at the 46th annual EAEG meeting, London.

Jakubowicz, H., Beasley, C., and Chambers, R., 1984, A comprehensive solution to problems in the processing of 3-D data: Presented at the 54th annual SEG meeting, Atlanta.

Judson D.R., Schultz, P.S., and Sherwood J.W.C., 1978, Equalizing the stacking velocities of dipping events via DEVILISH: Presented at the 48th annual international SEG meeting, San Francisco.

Larner, K.L., Hatton, L., Gibson, B., and Hsu, I-C., 1981, Depth migration of imaged time sections: Geophysics, **46**, 734-750.

Levin, F.K., 1971, Apparent velocity from dipping interfaces: Geophysics, **36**, 510-516.

Li, Z., Chambers, R., and Abma, R., 1987, Suppressing spatial aliasing noise in prestack Stolt f-k migration: Presented at the 57th annual SEG meeting, New Orleans.

Loinger, E., 1983, A linear model for velocity anomalies: Geophysical Prospecting, **31**, 98-118.

Luenberger, D.G., 1973, Introduction to linear and nonlinear programming: Addison Wesley.

Menke, W., 1984, Geophysical data analysis: discrete inverse theory: Academic Press.

Morley, L.C., Schneider, W.A., and Shurtleff, R.N., 1985, A comparative analysis of dip moveout and prestack migration: Presented at the 55th annual SEG meeting, Washington, D.C.

Neidell, N.S., and Taner, M.T., 1971, Semblance and other coherency measures for multichannel data: Geophysics, **36**, 482-497.

Nolet, G., ed., 1987, Seismic tomography: D. Reidel.

Press, W.H., Flannery, B.P., Teukolsky, S.A., and Vetterling, W.T., 1986, Numerical Recipes: Cambridge Univ. Press.

Rothman, D.H., Levin, S.A., and Rocca, F., 1985, Residual migration: applications and limitations: Geophysics, **50**, 110-126.

Schultz, P.S., and Claerbout, J.F., 1978, Velocity estimation and downward continuation by wavefront synthesis: Geophysics, **43**, 691-714.

Shurtleff, R.N., 1984, An F-K procedure for prestack migration and migration velocity analysis: Presented at the 46th annual EAEG meeting, London.

Stolt, R.H., 1978, Migration by Fourier transform: Geophysics, **43**, 23-48.

Stork, C., 1988, Ray trace tomographic velocity analysis of surface seismic reflection data: Ph.D. thesis, California Institute of Technology.

Stork, C., and Clayton, R.W., 1986, Case study of traveltime tomography applied to data sets containing lateral velocity variations: Presented at the 56th annual SEG meeting, in Houston.

Strang, 1980, Linear algebra and its applications: Academic Press.

Sword, C.H., 1987, Tomographic determination of interval velocities from reflection seismic data: the method of controlled directional reception: Ph.D. thesis, Stanford University (SEP-55).

Taner, T.M., and Koehler, F., 1969, Velocity spectra - digital computer derivation and application of velocity functions: Geophysics, **34**, 859-881.

Thorson, J.R., 1984, Velocity and slant stack inversion: Ph.D. thesis, Stanford University (SEP-39).

Thorson, J.R., and Claerbout, J.F., 1985, Velocity-stack and slant-stack stochastic inversion: Geophysics, **50**, 2727-2741.

Thorson, J.R., Gever, D.H., Swanger, H.J., Hadley, D.M., and Apsel, R.J., 1987, A model-based approach to interval velocity analysis: Presented at the 57th annual SEG meeting, New Orleans.

Tieman, H., 1984, Migration velocity analysis: theoretical development and practical results: Presented at the 54th annual SEG meeting, Atlanta.

Toldi, J.L., 1985, Velocity analysis without picking: Ph.D. thesis, Stanford University.

van der Made, P.M., van Riel, P., Hendricks, J.J.R., and Berkhout, A.J., 1987, Velocity-structure estimation by inversion of stacking information: Presented at the 49th annual EAEG meeting, Belgrade.

Yilmaz, O., and Claerbout, J.F., 1980, Prestack partial migration: Geophysics, **45**, 1753-1779.

Yilmaz, O., and Chambers, R., 1984, Migration velocity analysis by wave-field extrapolation: Geophysics, **49**, 1664-1674.

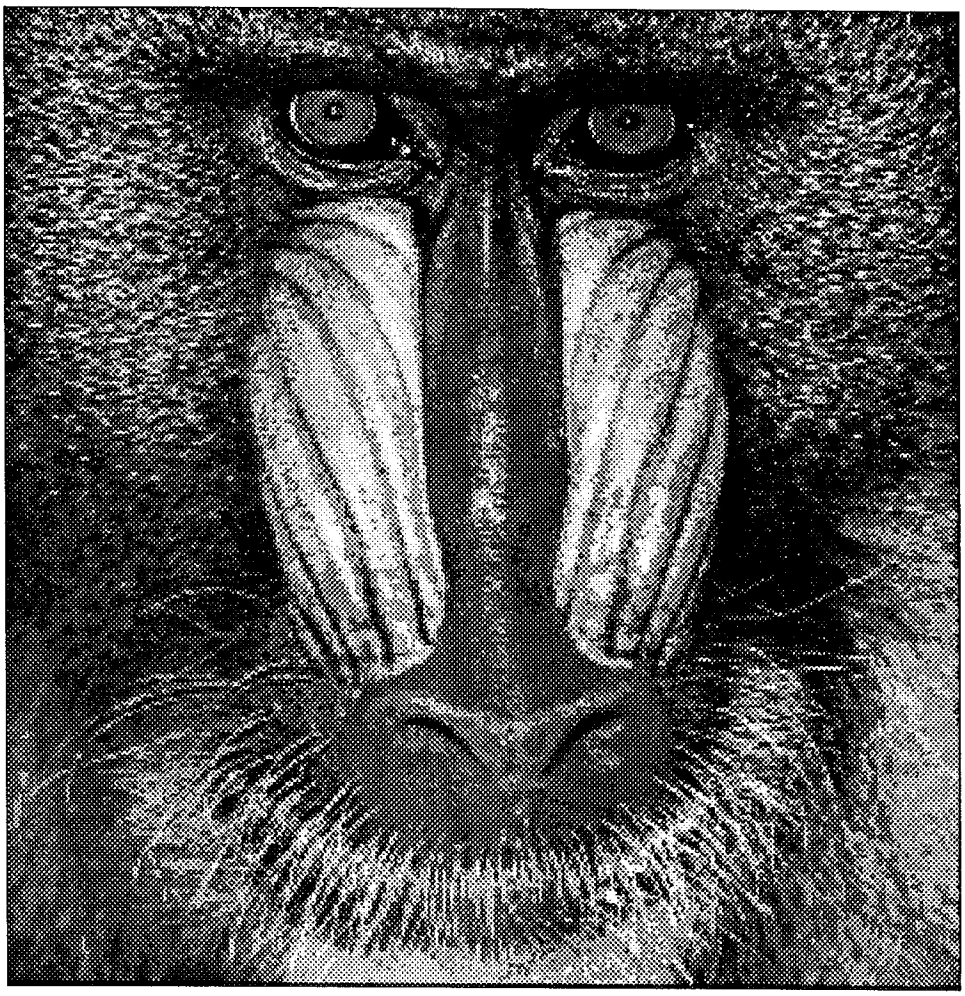

# WHEW!